https://doi.org/10.2352/ISSN.2470-1173.2021.2.SDA-011

Towards AO/EO Modulators in Lithium Niobate for Dual-Axis Holographic Displays

Mitchell Adams, Caitlin Bingham, Daniel Smalley; Brigham Young University; Provo, Utah

Abstract

A major limitation of acousto-optic (AO) modulator-based holographic displays is their inability to present full-parallax. We propose that full-parallax capabilities can be added to these displays by integrating electro-optic (EO) modulators into the architecture. We validated this concept by rendering computational models and by fabricating and testing EO deflection devices in lithium niobate. Our models suggest that an AO/EO modulator that yields an EO deflection range of 18.2° using less than 5 V can be fabricated given the limitations of standard photolithography and lithium niobate waveguides. Actual deflection ranges were measured from our fabricated devices and were compared to those that were derived from our model. In the worst case, the experimental results differed by about 16% compared to the corresponding theoretical result. In the best case, the error was smaller than our measurement tolerances. The work we have performed sets the stage for the first instance of an integrated electro-optic/acousto-optic modulator for holographic displays.

Introduction

The high cost, fabrication complexity, and sometimes bulky nature of spatial light modulators are a few of the characteristics that have restrained the widespread distribution of quality holographic video. An emerging technology that addresses many of the drawbacks of traditional SLMs is the acousto-optic (AO) modulator-based holographic display. These displays are monolithic, low cost, and simple to fabricate, requiring only two mask steps. They feature color multiplexing, no backplane, a high bandwidth, and the capacity to filter out unwanted light [1]. However, a limitation to the AO modulators used for these displays is that they cannot effectively scan along two orthogonal axes. This limits application to horizontal-parallax-only displays.

In this paper we propose a display that uses both acousto-optic (AO) and electro-optic (EO) modulators to enable dual-axis scanning while preserving the benefits of a single-axis AO modulator display.

We begin by unfolding the structure and operation of the modulators and display. We next present a series of simulations to explore the theoretical capacity of the proposed EO addition to the display. We also discuss our current work in fabricating EO modulator prototypes in lithium niobate to verify these results. Finally, we expound on the next steps towards fabricating a more optimal EO modulator that is compatible with the AO modulator for holographic displays.

Device Operation

In the following section we will first summarize the structure and operation of the AO modulator based display. We will then describe the modifications that will be made to integrate EO modulators into the architecture to enable dual-axis scanning. In this report we will designate the AO scanning direction as horizontal and the EO scanning direction as vertical.

AO modulators for horizontal-parallax displays

The basis of the AO modulator is an anisotropic material (typically lithium niobate) on which a waveguide is diffused, and on which an interdigital transducer (IDT) is deposited. The IDTs emit surface acoustic waves (SAWs) along the surface of the waveguide from one end, and light is injected into the waveguide from the other end. When the surface acoustic waves meet the propagating light, the light is ejected from the waveguide in the form of a leaky mode. (For this reason, these are also sometimes referred to as leaky-mode modulators.)

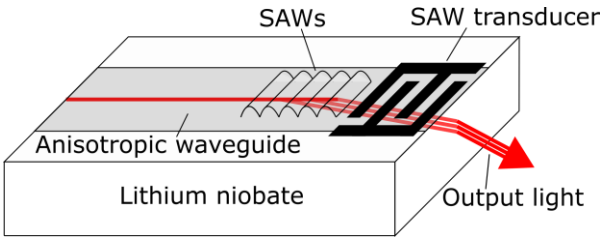

Figure 1. *Single channel AO-based leaky-mode modulator.*

The angle at which the light diffracts from the waveguide can be modulated by changing the frequency of the SAW signal. Not only can the light be steered, but it can also be horizontally focused by rapidly pulsing SAWs of different frequencies (see Figure 3a). By superimposing many SAWs, entire holograms are formed—holograms that can be modulated in real time.

A vertical array of these unit AO modulators can be integrated onto the same device to create a horizontal-parallax-only holographic display.

Additional modifications may enhance the quality of the display. For example, to avoid the limitations of an edge-emitting configuration, a grating can be integrated into the device that redirects the light out the front [2] or back [3] surface of the substrate. An expanded field of view may also be achieved through the use of diffractive orders from an internal grating [4] or by curving the substrate [5].

In this report we propose a modification that will bestow full-parallax capabilities on this display.

AO/EO modulators for full-parallax displays

To add vertical scanning capabilities to the leaky-mode device, the waveguide channel of the previously described modulator is divided into arrays of narrower subchannels (preferably single-mode subchannels). By modulating the relative phase of the light across the various subchannels, the subchannels act as a phased array that deflects the light vertically after it coincides with the SAWs and diffracts out of the waveguides. The phase modulation is achieved via the Pockels effect by inducing an electric field through the material from an overlaying electrode.

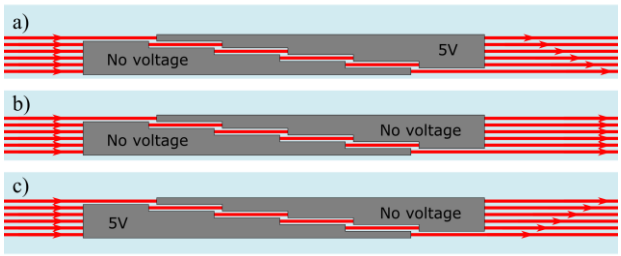

***Figure 2**. A variable voltage applied to an overlaying electrode can modulate the relative phase of light within the subchannels of an AO/EO modulator to cause the light to deflect by a given amount in a given direction as it diffracts out. These three figures illustrate modulation that will result in **a)** upward deflection, **b)** no deflection, and **c)** downward deflection. These figures assume that a grounding electrode is positioned on the opposite side of the waveguides.*

Just as pulsed SAW patterns are superimposed to generate horizontal accommodation, pulsed phased array patterns can be superimposed to enable vertical accommodation. When integrated onto a single device, the AO and EO modulators work together like two cylindrical lenses with adjustable focal lengths.

AO and EO modulators are highly cooperative in that both effects can be optimized simultaneously. For example, as the dimensions get smaller along one axis and longer along the other, both effects should improve. Furthermore, the introduction of the EO modulator should preserve most, if not all, of the benefits that the traditional leaky-mode modulator holds over pixelated modulators. For example, the modulation speed of an EO modulator can reach the excess of 100 GHz [6], which suggests that the EO modulators would be far from an impediment to the high temporal bandwidth of the leaky-mode display.

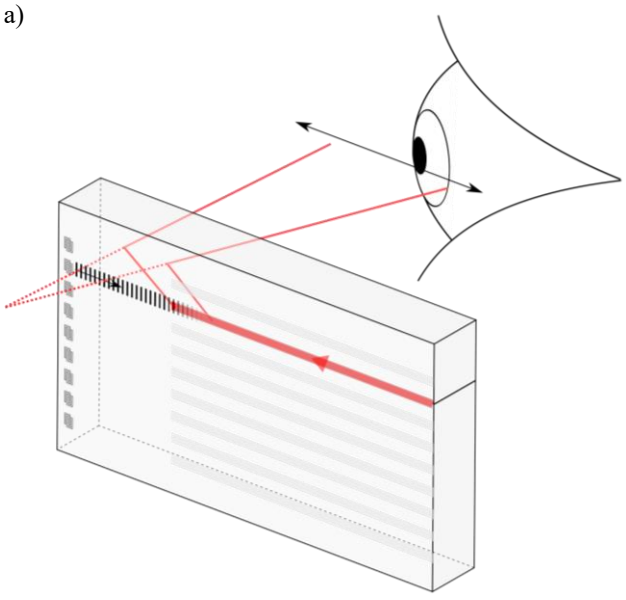

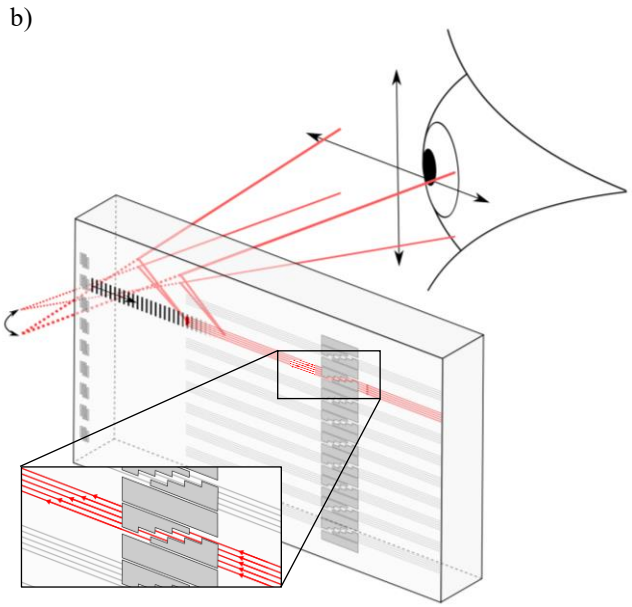

***Figure 3. a)** Surface-emitting AO modulator display with horizontal scanning capabilities. Two superimposed rays allow for horizontal accommodation. **b)** Surface-emitting AO/EO modulator with both horizontal and vertical scanning capabilities. Two vertical deflection orientations are shown here. The points of the two orientations at which horizontal focus occurs could be brought together to produce vertical focusing in addition to horizontal focusing.*

EO Modulator Theoretical Performance

The theoretical capacity of the proposed EO addition to the display was determined using analytical models, including a Fraunhofer model to simulate diffraction. We present these results and use them to down-select a set of parameters for a theoretically optimal EO modulator.

The parameters that most affect the performance of the EO modulator include the widths of the waveguide subchannels, the separation distance of the waveguide subchannels, the number of waveguide subchannels making up the phased array, the electrode interaction length, and the electrode plate separation distance. The following figure illustrates what is signified by these parameters.

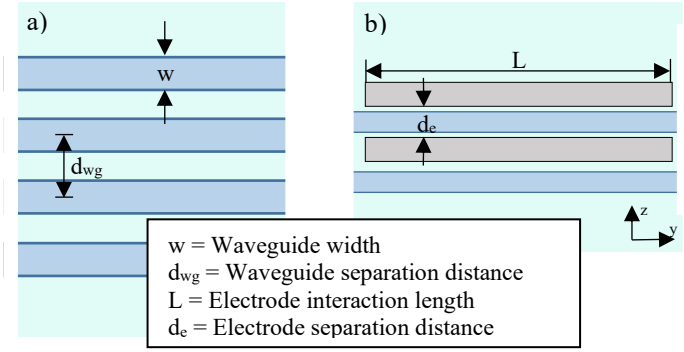

***Figure 4. a)** Slice of a unit EO modulator with four subchannels. The waveguide width is defined as the lateral width of a single subchannel. The waveguide separation distance is defined as the lateral distance between the center of one subchannel and the center of an adjacent subchannel. **b)** Slice of a EO modulator with two subchannels and laterally positioned electrodes. The electrode interaction length is the length of the electrode along the direction of propagation of the waveguide. The electrode plate separation distance is the distance from one electrode to the other in the r_{33} direction.*

Two outputs of the EO modulator system which we deemed particularly important, and which we present here, are deflection angle and beam quality.

Modeled Deflection Angle

An important parameter for holographic displays is the field of view. The field of view is limited in part by the maximum deflection angle of the light modulators. Thus, to increase the vertical field of view of our display, the deflection angle of our EO modulator should be maximized.

The maximum permissible EO deflection angle in a given direction is the angle at which light deflects when the relative phase between adjacent waveguides is modulated by a half-wavelength. We will refer to this angle as the half-wave deflection angle.

Since the light can be modulated a half-wavelength in either direction, the total permissible field of view that can be obtained from these modulators in their raw form is twice the half-wave deflection angle (although the image quality may be compromised near this half-wave threshold).

Modeled Deflection Angle as a Function of Waveguide Separation

The parameter that most affects this half-wave deflection angle is the separation distance between waveguides. Figure 5 reveals that the half-wave deflection angle increases exponentially as the waveguide separation is made smaller. Thus, to maximize the half-wave deflection angle, the waveguide separation distance should be made as small as possible.

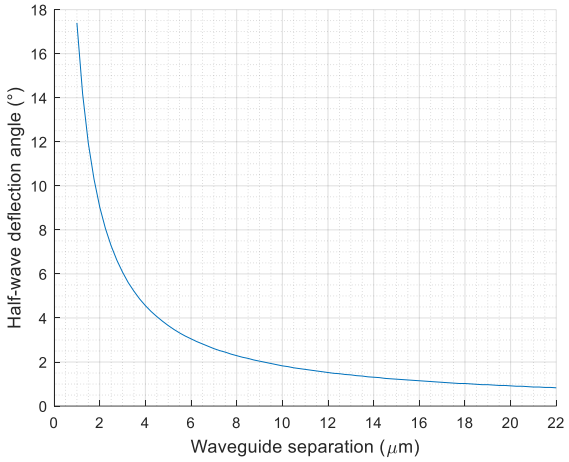

Figure 5. *Half-wave deflection angles for EO deflectors of various waveguide separation distances derived from an analytical Fraunhofer model. The half-wave deflection angle is defined as the angle that light deflects relative to rest when the phases of adjacent waveguides are a half wavelength apart. The waveguide separation distance is defined as the lateral distance between the center of two adjacent waveguides. Assumes 640 nm wavelength light.*

How small the separation distance can be is limited by the waveguide width and the resolution of the fabrication equipment.

Waveguide width is a limiting factor because the separation distance, as it is defined in Figure 4, cannot be made smaller than the waveguide width, lest the waveguides overlap.

We performed finite difference simulations that suggest that the minimum permissible width of a 0.6 μm deep proton exchange waveguide in lithium niobate may be less than 250 nm when illuminated with 640 nm light. This will likely not be the limiting factor in narrowing the waveguides

Narrow lithium niobate waveguides fabricated using proton exchange can be lossy. With too much loss, the lossy light becomes noticeable and distracting. The intensity of the light of interest also diminishes.

We must account for the fact that it is difficult to consistently fabricate features smaller than about 1 μm using standard photolithography.

One final consideration when bringing two waveguides close together for an extended length is the presence of crosstalk.

Assuming sufficiently low-loss and inconsequential crosstalk, we believe that 1-1.5 μm wide waveguides with 2 μm separation distances can be reasonably achieved under most low-cost fabrication settings.

Our model suggests that a 2 μm separation would result in a 9.1° half-wave deflection angle, or an 18.2° deflection range.

Modeled Deflection Angle as a Function of Electrode Parameters

Though the maximum deflection angle is limited by the waveguide structure, the amount of deflection that occurs within that range is determined by the electrode parameters, including the electrode interaction length, the electrode separation distance, and the applied voltage. Equation 1 can be used to predict the deflection, θ, that occurs for a given applied voltage and electrode structure:

$$\theta = \frac{\theta_\pi n_e^3 r_{33} \Gamma_{wg} V L}{\lambda d_z (N-1)} \quad (1)$$

In this equation, θ_π represents the half-wave deflection angle, n_e is the effective index of refraction, r_{33} is the is the electrooptic coefficient, Γ_{wg} is the overlap correction factor (which accounts for when the electrical and optical fields do not overlap completely), V is the applied voltage, L is the electrode interaction length, λ is the wavelength, and d_z is the electrode separation distance in the z direction.

According to this equation, the deflection angle increases linearly with increased electrode interaction length and decreased plate separation distance. These parameters can be designed to allow for the desired amount of deflection (within the half-wave angle threshold) for a given applied voltage. An example case could be that the electrodes are positioned 15 μm apart in the z direction and span 5 mm along the direction of propagation. For a two-subchannel modulator, this would yield a deflection range that could be controlled using less than 5 V.

N in this equation represents the number of waveguides in a unit modulator, suggesting that the required voltage to achieve a given deflection angle is inversely proportional to the number of subchannels. The equation assumes that the electrode interaction length, L, pertains to the longest electrode span which typically covers the top or bottom subchannel and that the electrodes get consistently smaller as they approach the subchannel on the opposite end, which has no electrode covering (as illustrated in Figure 2). In other words, each subchannel in the unit modulator needs to have an identical phase difference from its neighboring subchannels.

Alternatively, more complex design and control could enable the modulator to be controlled within the half-wave voltage no matter how many subchannels are used. Since phase is periodic, any phase difference could be represented within -π and π. But this would require individual control of the phase in each subchannel, thus complicating the fabrication, design, and control.

Modeled Beam Quality

Another quality of interest in our EO modulator design is the output beam quality. Ideally, the majority of the light from the EO modulator should be concentrated into the central, zero-order fringe. This was not the case for the initial EO modulators we fabricated as illustrated in the far field pattern from one of these modulators shown in Figure 6a. Figure 6b shows a simulated far field pattern corresponding to an EO modulator that incorporates the optimizations described in this section.

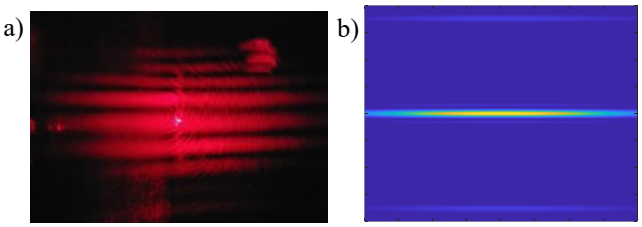

Figure 6. a) *Far field pattern from an unoptimized EO modulator fabricated in our lab.* ***b)*** *Computational model showing how the far field patterns could look after incorporating the optimizations described in this section.*

Increasing diffraction efficiency

Our first task towards improving the beam quality will be to increase the zero-order diffraction efficiency. A simple way to do this is to increase the width of the waveguide subchannels such that they approach the separation distance (recall that the separation distance must be larger than the waveguide width according to our definitions).

Figure 7 demonstrates this effect qualitatively by showing far field diffraction patterns from simulated EO modulators that are composed of two subchannels separated by 4 µm. In each case, the waveguide width increases. As the waveguide width approaches the separation distance (i.e. as the gap between subchannels approaches 0 µm), more light is concentrated into the zero-order fringe.

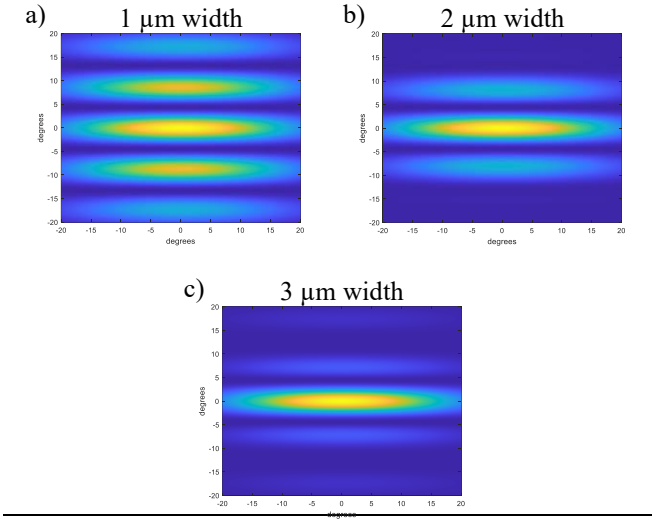

Figure 7. *Far field diffraction patterns from EO modulators that are composed of two waveguide subchannels separated by 4 µm and with waveguide widths of* ***a)*** *1 µm,* ***b)*** *2 µm, and* ***c)*** *3 µm. Note that these images are normalized, meaning that relative intensities do not translate from image to image.*

The effect described in this section of increasing the waveguide width to be closer to the separation distance holds for any separation distance. Figure 8 shows the case of two 1.5 µm wide subchannels separated by 2 µm is comparable.

Reducing the beam span

Another interesting observation that can be made by comparing the far field pattern in Figure 8 to the patterns in Figure 7 is that in Figure 8 the fringes spread out over a wider angular span. This trend is true in general: smaller separation distances produce larger beam spans. For holographic displays, a more concentrated beam is typically preferrable.

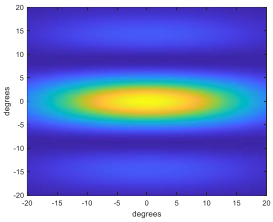

Figure 8. *Far field diffraction pattern from an EO modulator with two 1.5 µm wide subchannels separated by 2 µm. Decreasing the separation distance is necessary for increasing the half-wave deflection angle (see Figure 5). But by decreasing the separation distance, the zero-order fringe also becomes less condensed.*

This presents two conflicting interests. We want to maximize the deflection angle, which is achieved by decreasing the separation distance (Figure 5). But decreasing the separation distance increases the vertical beam span, which we do not want.

A solution to this conundrum is to increase the number of subchannels in a unit EO modulator. By increasing the number of subchannels, the vertical span of the zero-order fringe is condensed while still preserving the half-wave deflection angle. This effect is illustrated by the series of simulated far field diffraction patterns shown in Figure 9. In these simulations, the number of subchannels is increased from two to sixteen while the widths and separation distances of the waveguides are kept constant.

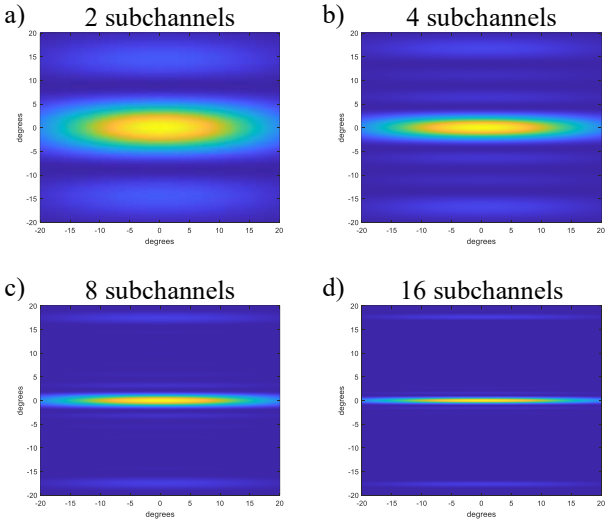

Figure 9. *Simulated far field diffraction patterns from EO modulators that are composed of* ***a)*** *two,* ***b)*** *four,* ***c)*** *eight, and* ***d)*** *sixteen subchannels that are 1.5 µm wide and separated by 2 µm. Note that these images are normalized, meaning that relative intensities do not translate from image to image.*

As described earlier in this report, a drawback of an increased number of waveguides is that either an increased amount of voltage or a more complicated system is required.

The optimal number of subchannels per unit modulator ultimately depends factors relevant to the specific application such as the distance of the display from the viewer (angular span maps to a larger linear distance as the light projects further away), the desired optical efficiency, and the maximum supply voltage.

Single-mode waveguides

The waveguides should be restricted to a single mode for optimal beam quality. This is another argument for using narrow waveguides. Our finite difference simulations suggest that a 0.6 µm deep rectangular proton exchange waveguide in lithium niobate should be narrower than 0.7 µm to be single-mode.

As it is difficult to fabricate low-loss waveguides that are this narrow, especially using standard photolithography, one might opt for quasi-single-mode waveguides. A 1.5 µm wide waveguide supports three modes, according to our simulation.

Summary

In this section we have discussed the effect that various parameters have on EO modulator performance for holographic displays. A summary of our findings is found in Table 1.

Table 1. Summary of EO modulator parameters and their effect on performance

Parameter (see Figure 4)	Optimal value	Effect on performance
Waveguide separation distance	As small as possible. 2 µm should be feasible under most fabrication settings.	Smaller separation distances lead to larger half-wave deflection angles but increase the vertical span of fringes
Waveguide width	As close to the separation distance as possible. 1-1.5 µm should be feasible under most fabrication settings	Narrower widths permit smaller separation distances. Narrower widths also decrease the number of modes. Larger widths relative to the separation distance increase diffraction efficiency
Number of waveguides per unit modulator	Depends on the application	More waveguide subchannels lead to smaller vertical fringe spans but requires a higher voltage or a more complex design
Electrode interaction length	As long as the structure allows	Larger interaction length leads to more modulation per volt
Electrode separation distance	As close as possible	Smaller separation distance leads to more modulation per volt

Performance of Basic EO Modulator Prototypes in Lithium Niobate

As an initial proof of concept of the EO modulator in lithium niobate for AO/EO displays, we fabricated a series of basic EO modulator-based deflectors. We measured the half-wave deflection angle and the half-wave voltage and compared the results to the theoretical values.

Structure

Our original EO testing prototypes were structurally similar to an integrated Mach-Zehnder Interferometer. The key difference was that the waveguide branches did not merge back together; rather, they were brought to close proximity at the polished substrate edge. At the polished edge the light in the two waveguides diffracted out into free space in a double-slit-like pattern.

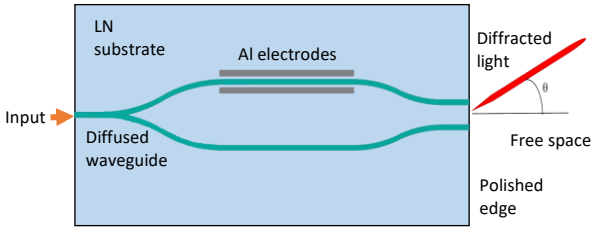

Figure 10. *EO modulator prototype with two subchannels used for initial deflection tests.*

Since our waveguides were y-propagating in x-cut lithium niobate, the strongest electro-optic effects were achieved when the electric field ran laterally across the waveguide (in the z direction). We achieved this by depositing two aluminum electrodes on either side of one of the waveguide branches.

Results

Half-wave deflection angle as a function of waveguide separation distance

We fabricated several EO deflection devices with varying parameters. Figure 11 shows the half-wave deflection angle of four of these devices as a function of waveguide separation distance.

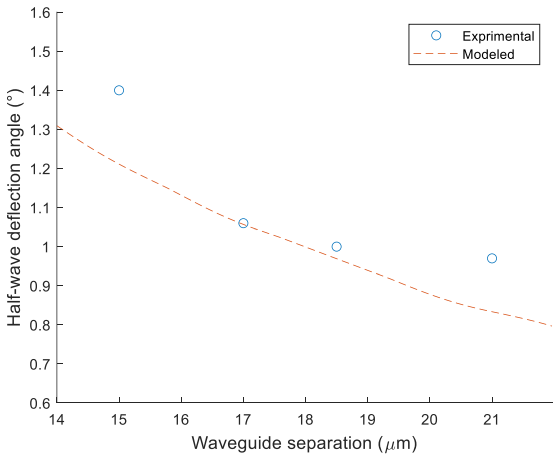

Figure 11. *Half-wave deflection angle as a function of waveguide separation distance for an EO modulator prototype in lithium niobate and compared to the modeled values.*

In the worst case, the experimental result differed by about 0.2°, or 16%, compared to the corresponding theoretical result. In the best case, the difference was smaller than we could measure. The discrepancies can likely be attributed to errors in measurement, both of the device parameters and of the deflection angle.

Optimization and Integration

Our next steps will be to further optimize our EO modulator in accordance with the parameters from Table 1, and also to integrate it into the leaky-mode modulator as described in Device Operation. In this section we will elaborate on some of the specific challenges relevant to these next implementations.

Optimized diffusion for narrower waveguides

To achieve waveguides that are closer together, we will need to fabricate narrower waveguides. (The width of the waveguides must be smaller than the separation distance or the waveguides will overlap.) To fabricate narrower waveguides, a low-loss waveguide diffusion technique must be used.

The prototypes presented in this report used a modified annealed proton exchange (APE) diffusion method which enabled waveguides as narrow as about 8 μm to pass enough light through to accomplish their purpose.

A recent test we carried out revealed that a soft proton exchange (SPE) diffusion technique (3% lithium benzoate dilution, diffused at 275° C) produces 5 μm wide waveguides that exhibit around 4 dB/cm loss, which is about an 85% loss reduction from the APE method we were using before. This level of loss suggests that waveguides even narrower than 5 μm could be fabricated using SPE.

Reverse proton exchange (RPE) is another technique that may produce low-loss waveguides.

SPE and RPE are both superior to APE in the preservation of nonlinear properties [7,8].

Transition to z-cut lithium niobate for simpler electrode fabrication

As the waveguides are made narrower and are brought closer together, it will become increasingly difficult to pattern long, narrow electrodes that fit in between the waveguides as required for EO modulators in x-cut lithium niobate (see Figure 10 and reference [9]).

An electrode structure that would be easier to consistently fabricate is illustrated in Figures 2 and 3a. For this structure, a contiguous conductor is patterned across all of the subchannels of a unit modulator and sends an electric field down into the waveguide from the top. In order to take advantage of the strong r_{33} electro-optic coefficient, z-cut lithium niobate should be used in this case.

There are at least two considerations in switching to this electrode structure. First, a metallic electrode cannot be placed directly on top of a waveguide, lest the electrode absorb the light from the waveguide. Either a transparent buffer layer needs to be placed in between the electrode and the waveguide (typically made of SiO_2) or a non-metallic electrode needs to be used, such as indium tin oxide or graphene [10].

The other consideration is the position of the grounding electrode. For z-cut EO modulators in lithium niobate, the grounding electrode is typically placed on top of the substrate adjacent to the other electrode [11]. This does not result in all of the electric field being targeted exactly downward through the waveguide, meaning the Γ_{wg} term in Equation 1 would be diminished. Nonetheless, grounding plates could be placed on either side of a unit modulator, meaning the distance from a grounding plate to a subchannel would be just over half the width of the unit modulator, on average. This distance is small enough that it may overcome the effects of the deprecated Γ_{wg} value, according to Equation 1.

An alternative solution could be to use a thin lithium niobate substrate and to place the grounding electrode on the bottom of the substrate. We have successfully fabricated the optical components of an EO modulator on a substrate as thin as 100 μm, though it is difficult due to their fragile nature. While 100 μm is a larger electrode separation distance than what would be possible in the previous method, the electric field in this case would run directly down through the waveguide.

Multichannel arrays

The transition to a multichannel array presents the added challenge of dividing the light into more than two subchannels while preserving the relative phase across subchannels. Assuming enough room is available on the substrate, a tree of y-branches or multimode interferometers might be used. A star coupler is another option.

Integration into AO/EO modulator

As we integrate the AO and EO modulators together into a single device, the aspects that will be different from anything we have tested are 1) the leaky-mode effect from a group of subchannels rather than a single channel, and 2) phased array diffraction stemming from the leaky-mode and diffracting down into the substrate rather than directly out of the edge of the substrate. Since we have not tested these things previously, it is possible that we will encounter unanticipated behavior.

The physical implementation of this AO/EO device is to be reported on in a future work.

Conclusion

This research has set the stage for a joint AO/EO holographic display. While both AO and EO integrated deflection devices have been independently reported in previous literature, we know of no research that integrates them together in one, particularly as a medium for holographic displays.

We have reported on modeled results that demonstrate the capacity of the proposed EO modulator addition. Our models show that we can independently control the half-wave deflection angle, the zero-order diffraction efficiency, and the vertical span of the diffracted fringes by optimizing the number of waveguides in a unit modulator, the waveguide widths, and the waveguide separation distances. We can determine the amount of deflection that occurs per applied volt through the electrode structure. Using low-cost photolithography techniques, AO/EO modulators in their raw form could be fabricated that, according to these models, yield EO deflection ranges larger than 18°. The electrode structure can be designed to allow for this full deflection range to controlled using less than 5 volts for a two-channel modulator.

We fabricated a simple EO modulator in x-cut lithium niobate and compared its half-wave deflection angle with the modeled values. We found that in the worst case, the experimental result differed by about 0.2°, or 16%, compared to the corresponding theoretical result. In the best case, they were nearly identical.

Our next tasks will be to 1) optimize our EO modulator for holographic displays based on the results from our model, and 2) integrate the EO modulator into the leaky-mode architecture to form a dual-axis AO/EO modulator.

References

[1] D.E. Smalley, Q.Y.J. Smithwick, V.M. Bove, J. Barabas, and S. Jolly, “Anisotropic leaky-mode modulator for holographic video displays,” Nature, vol. 498, no. 7454, pp. 313-317, 2013.

[2] J. C. Perkinson, M. G. Moebius, E. J. Brundage, W. A. Teynor, S. J. Byrnes, J. C. Hsiao, W. D. Sawyer, D. M. Callahan, I. W. Frank, J. J. LeBlanc, and G. E. Favalora, "Surface-emitting electroholographic SAW modulator," Opt. Express, vol. 28, no. 2, pp. 1585-1594, 2020.

[3] S. McLaughlin, A. Henrie, S. Gneiting, and D. E. Smalley, "Backside emission leaky-mode modulators," Opt. Express, vol. 25, no. 17, pp. 20622-20627, 2017.

[4] D. Pettingill, D. Kurtz, D. Smalley, "Static Structures in Leaky Mode Waveguides," Appl. Sci., vol. 9, no. 2, p. 247, 2019.

[5] J. C. Leach, D. Smalley, “Considerations of Curvature for a Near-Eye Holo-Video Display,” Appl. Sci., vol. 10, no. 19, p. 6888, 2020.

[6] M. J. Fitch, *Laser Spectroscopy for Sensing*, Woodhead Publishing Limited, 2014.

[7] L .Chanvillard, P. Aschiéri, P. Baldi, D. B. Ostrowski, M. de Micheli, L. Huang, and D. J. Bamford, “Soft proton exchange on periodically poled LiNbO3: A simple waveguide fabrication process for highly efficient nonlinear interactions,” Appl. Phys., vol. 76, no. 9, pp.1089-1091, 2000.

[8] K. R. Parameswaran, R. K. Route, J. R. Kurz, R. V. Roussev, M. M. Fejer, and M. Fujimura, “Highly efficient second-harmonic generation in buried waveguides formed by annealed and reverse proton exchange in periodically poled lithium niobate,” Opt. Lett, vol. 27, no. 3, pp. 179-181, 2002.

[9] L. LaComb, Jr., A. Bablumyan, R. Rankin, A. Ordyan, V. M. Bove Jr., S. Jolly, B. Datta, V. Parthiban, T. Schoeppner, D. Smalley, and D. Barton,. “Acousto-Optic and Electro-Optic Waveguide Fabrication” in “Leaky Waveguide Full Parallax Holographic Video Display (LWFP-HVD) Phase I.,” pp. 17-19, 2019.

[10] Z. Chang, W. Jin, and K. S. Chiang, “Graphene electrodes for lithium-niobate electro-optic devices,” Opt. Lett, vol. 43, no. 9, pp. 1718-1721, 2018.

[11] D. Janner, D. Tulli, M. Belmonte, and V. Pruneri, “Waveguide electro-optic modulation in micro-engineered LiNbO3,” J. Opt. A: Pure Appl. Opt., vol. 10, no. 10, 2008

Author Biographies

Mitchell Adams and Caitlin Bingham are graduate and undergraduate students respectively in the Electrical and Computer Engineering Department at Brigham Young University. Their research focuses on waveguide based holographic video displays.

Daniel Smalley received his BS, MEng, MS, and PhD degrees from Massachusetts Institute of Technology. He is currently an associate professor in the Electrical and Computer Engineering Department at Brigham Young University. His main research focus is on the development of novel holographic and volumetric displays.

JOIN US AT THE NEXT EI!

IS&T International Symposium on

Electronic Imaging

SCIENCE AND TECHNOLOGY

Imaging across applications . . . Where industry and academia meet!

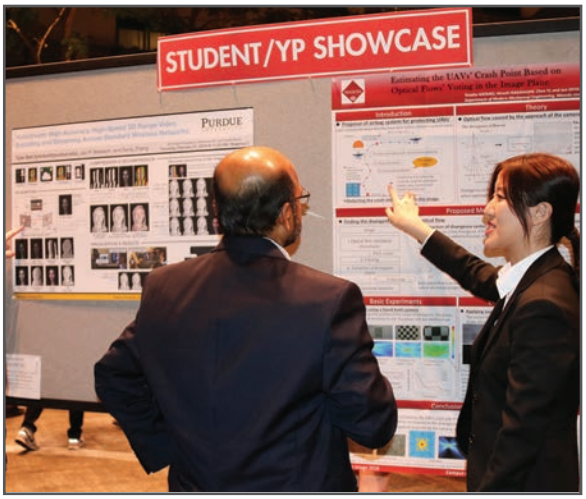

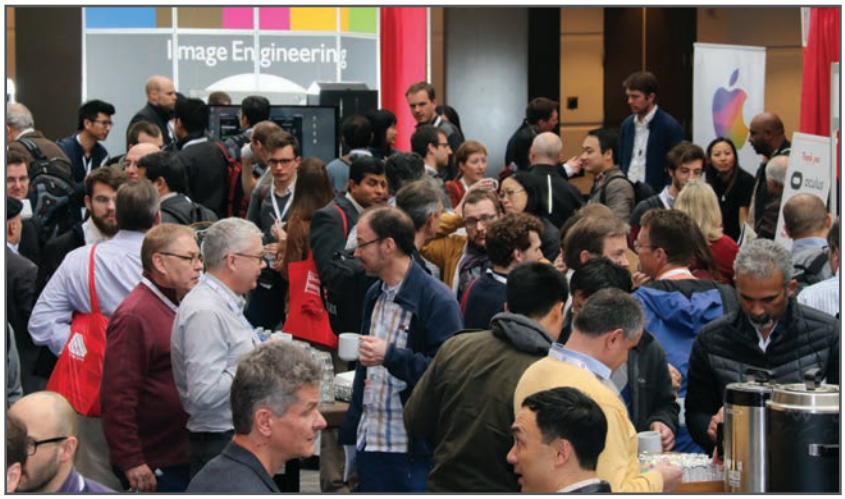

• SHORT COURSES • EXHIBITS • DEMONSTRATION SESSION • PLENARY TALKS •
• INTERACTIVE PAPER SESSION • SPECIAL EVENTS • TECHNICAL SESSIONS •

www.electronicimaging.org

IS&T
imaging.org